Acta Oceanol. Sin., 2021, Vol. 40, No. 5, P. 114–119
https://doi.org/10.1007/s13131-021-1728-z
http://www.hyxb.org.cn
E-mail: ocean2@hyxb.org.cn

Glacial bedforms in the Northwind Abyssal Plain, Chukchi Borderland

Zhongyan Shen[1, 2†], Tao Zhang[1, 2†], Jinyao Gao[1, 2], Chunguo Yang[1, 2*], Qingsheng Guan[1, 2, 3]

[1] Key Laboratory of Submarine Geosciences, Ministry of Natural Resources, Hangzhou 310012, China

[2] Second Institute of Oceanography, Ministry of Natural Resources, Hangzhou 310012, China

[3] School of Geographic and Oceanographic Sciences, Nanjing University, Nanjing 210023, China

Received 1 April 2020; accepted 3 June 2020

Abstract

A series of sub-parallel linear glacial scours are identified on the crest of the Baoshi Seamount in the Northwind Abyssal Plain by compiling new multibeam data acquired during the 9th Chinese Arctic Research Expedition (CHINARE-Arc9) in 2018 and previously published data. The new data reveal scours that developed at water depths of 850–1 030 m with an orientation of about 75°/255°. The maximum water depth occurs in the southernmost scour and is deeper than that from previous investigations, which showed a maximum scouring depth of about 900 m on the seamount. The topographic and geomorphological characteristics suggest that these scours resulted from erosion by the ice shelf extending from the Chukchi margin and/or Laurentide Ice Sheet that grounded on the crest of the seamount and moved in a NE–SW direction. Other possibilities of their genesis include armadas of large icebergs/multi-keel icebergs calved from the Chukchi Shelf or the Laurentide Ice Sheet. The new data provide new constraints for assessing the extent and volume of the ice sheet in the Chukchi area during glacial maxima.

Key words: Chukchi Borderland, Northwind Abyssal Plain, glacial bedforms, mega-scale glacial lineations, ice shelf

Citation: Shen Zhongyan, Zhang Tao, Gao Jinyao, Yang Chunguo, Guan Qingsheng. 2021. Glacial bedforms in the Northwind Abyssal Plain, Chukchi Borderland. Acta Oceanologica Sinica, 40(5): 114–119, doi: 10.1007/s13131-021-1728-z

1 Introduction

The ice conditions of the Arctic Ocean during Pleistocene glacial maxima are highly controversial. Extreme viewpoints vary from an ice-free condition (Donn and Ewing, 1966) to a thick ice shelf covering the Arctic Ocean (e.g., Mercer, 1970; Hughes et al., 1977; Jakobsson et al., 2016). The direct geological evidence of the latter is the numerous submarine erosional bedforms formed by ice shelf grounding on bathymetric highs in the central Arctic Ocean, such as the Mendeleev Ridge, the Lomonosov Ridge, and the Chukchi Borderland (Niessen et al., 2013; Stein et al., 2010; Jakobsson, 1999; Polyak et al., 2001; Jakobsson et al., 2008, 2016; Dove et al., 2014). These erosional bedforms suggest that the maximum thickness of the ice shelf can exceed 1 km (Jakobsson et al., 2016). An alternative view is provided by Kristoffersen et al. (2004), who suggested that armadas of large icebergs disintegrated from land-based ice sheets could also cause such bedforms. These deep-water glacial bedforms not only constrain the extent of the Arctic ice shelf in geological history, but also provide direct observational data for estimating the maximum ice volume around the Arctic Ocean during glacial maxima.

Along the Chukchi continental margin, thick glacial deposits revealed by multi-channel seismic data indicate a long history of glaciation (Hegewald, 2012; Hegewald and Jokat, 2013). Although there are some early views suggesting almost no ice at the Chukchi continental margin during the Pleistocene (e.g., Ehlers and Gibbard, 2007), many studies have revealed a variety of glacial bedforms in this region (Fig. 1). Borehole dating of glacial bedforms on the southernmost Northwind Ridge reveals two recent phases of glaciations, possibly during MIS 2 and MIS 4 to 5d (Polyak et al., 2007). Some studies have even proposed an ice sheet capping the Chukchi margin during previous glacial maxima, implying an ice shelf extending beyond the Chukchi Shelf break (Polyak et al., 2001; Dove et al., 2014). However, the extent and maximum thickness of such an ice sheet/ice shelf are not well established. In areas shallower than 700 m water depth of the Chukchi Borderland, many glacial bedforms, such as mega-scale glacial lineations (MSGLs) and morainic ridges, have been discovered (Polyak et al., 2001; Jakobsson et al., 2008; Dove et al., 2014). However, in deeper water, only a few glacial erosional bedforms have been found (Jakobsson et al., 2008; Dove et al., 2014). One typical example is the streamlined bedforms found at about 900 m water depth on the crest of a seamount located at about 75.5°N (called the "Baoshi Seamount" in this paper) in the Northwind Abyssal Plain (NAP) (called MSGLs in Dove et al., 2014). MSGLs are representative bedforms beneath ice streams (e.g., Shipp et al., 1999; King et al., 2009) and are widely found in cross-shelf troughs on glaciated continental shelves (Ottesen and Dowdeswell, 2009). Similar streamlined bedforms are observed on the submarine highlands away from the wide continental shelf, attributed to the grounding of ice shelves and icebergs (e.g., Polyak et al., 2001; Kristoffersen et al., 2004) instead of ice streams. Obviously, when restoring the extent and thickness of the possible ice sheet/ice shelf in the Chukchi area, it is vital to identify whether these streamlined bedforms are caused by ice

Foundation item: The National Natural Science Foundation of China under contract No. 41976079; the Chinese Polar Environment Comprehensive Investigation and Assessment Programmes under contract No. CHINARE-03-03.

*Corresponding author, E-mail: yangchunguo@sio.org.cn

†These authors contributed equally to this work.

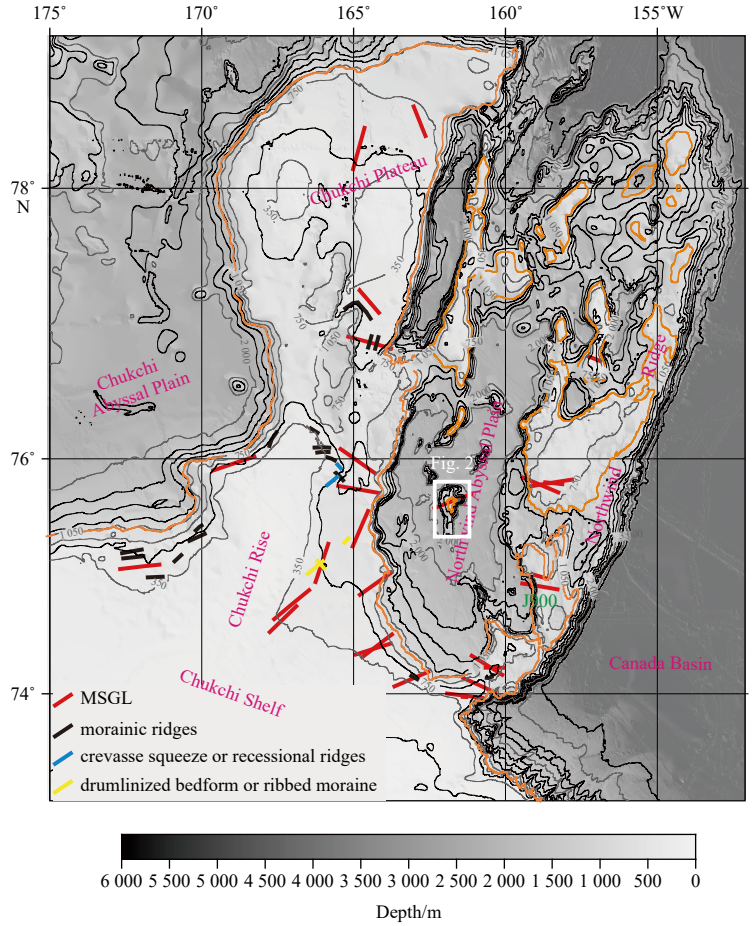

Fig. 1. Bathymetry and submarine glacial bedforms of the Chukchi Borderland. The bathymetric grid is from IBCAO V3.0 (Jakobsson et al., 2012). Glacial bedforms are marked with thick lines of different colors, and all of them are drawn according to Dove et al. (2014), Jakobsson et al. (2008) and Polyak et al. (2001). The white rectangle is the area in Figs 2a, c and d (the Baoshi Seamount). The 1 050-m isobath is marked with a thick yellow line for reference. J900 represents the MSGLs identified by Jakobsson et al. (2008) at a water depth of approximately 900 m.

shelf or icebergs. Nevertheless, Dove et al.'s (2014) multibeam data on the Baoshi Seamount only reveal part of the bedforms (Fig. 2b) whose origin is questionable. In this paper, a bathymetric grid that fully covers the Baoshi Seamount using newly acquired and previously published multibeam data (Dove et al., 2014) is presented. With this approach, the objectives of this paper are: (1) to determine the genesis and ice source of these subparallel linear glacial scours on the Baoshi Seamount; (2) to provide geological constraints for restoring the extent and volume of ice in the Chukchi area during glacial maxima.

2 Study area and methods

The NAP is a N–S trending flat valley between the Chukchi Plateau-Chukchi Rise in the west and the Northwind Ridge in the east (Hall, 1990) (Fig. 1). It is an extensional basin formed during the late Paleocene (Grantz et al., 2011) or the latest Cretaceous–late Paleocene (Ilhan and Coakley, 2018). The Baoshi Seamount is one of the seamounts in the NAP close to the Chukchi Shelf, and the water depth at its top is less than 1 000 m (Figs 1 and 2).

The multibeam data used in this paper were primarily acquired by an ELAC SeaBeam 3020 ICE echo sounder mounted on the R/V *Xuelong* during the 9th Chinese Arctic Research Expedition (CHINARE-Arc9) in the summer of 2018. In the Baoshi Seamount area (the white rectangle in Fig. 1), the surveyed water depths range from about 2 200 m to 850 m, and the swath width is about 2 times the water depth. The survey lines are roughly E–W (Fig. 2a). The bathymetric survey of CHINARE-Arc9 is complementary to previous investigations in this area (e.g., Dove et al., 2014) and explores more detailed bedforms on this seamount.

The multibeam data acquired during CHINARE-Arc9 were processed by CARIS HIPS software. After processing was completed, a grid with a cell size of 50 m was generated (Fig. 2c), and the data were exported as Generic Sensor Format (GSF). At the same time, open source software MB-System (Caress and Chayes, 2017) was used to edit the historical multibeam data from four cruises in the study area shared by the US National Geophysical Data Center (NGDC), including HLY0302, HLY0404 and HLY0703, by the US Coast Guard's Icebreaker *Healy* in 2003, 2004 and 2007, respectively, and MGL1112 by R/V *Marcus G. Langseth* in 2011. These open-access multibeam data are combined with the new data from CHINARE-Arc9, and consequently, a compiled grid with a cell size of 50 m is generated (Figs 2a and d). The combined data enable a nearly full illustration of the study area, revealing much more complete glacial bedforms than in the past. In the quantitative topographic analyses, if the bedforms are within the data extent of the CHINARE-Arc9 grid, the CHINARE-Arc9 grid is used with a higher priority. Otherwise, the compiled grid is used.

3 Geomorphological characteristics and glacial bedforms of the Baoshi Seamount

The compiled multibeam grid shows that the Baoshi

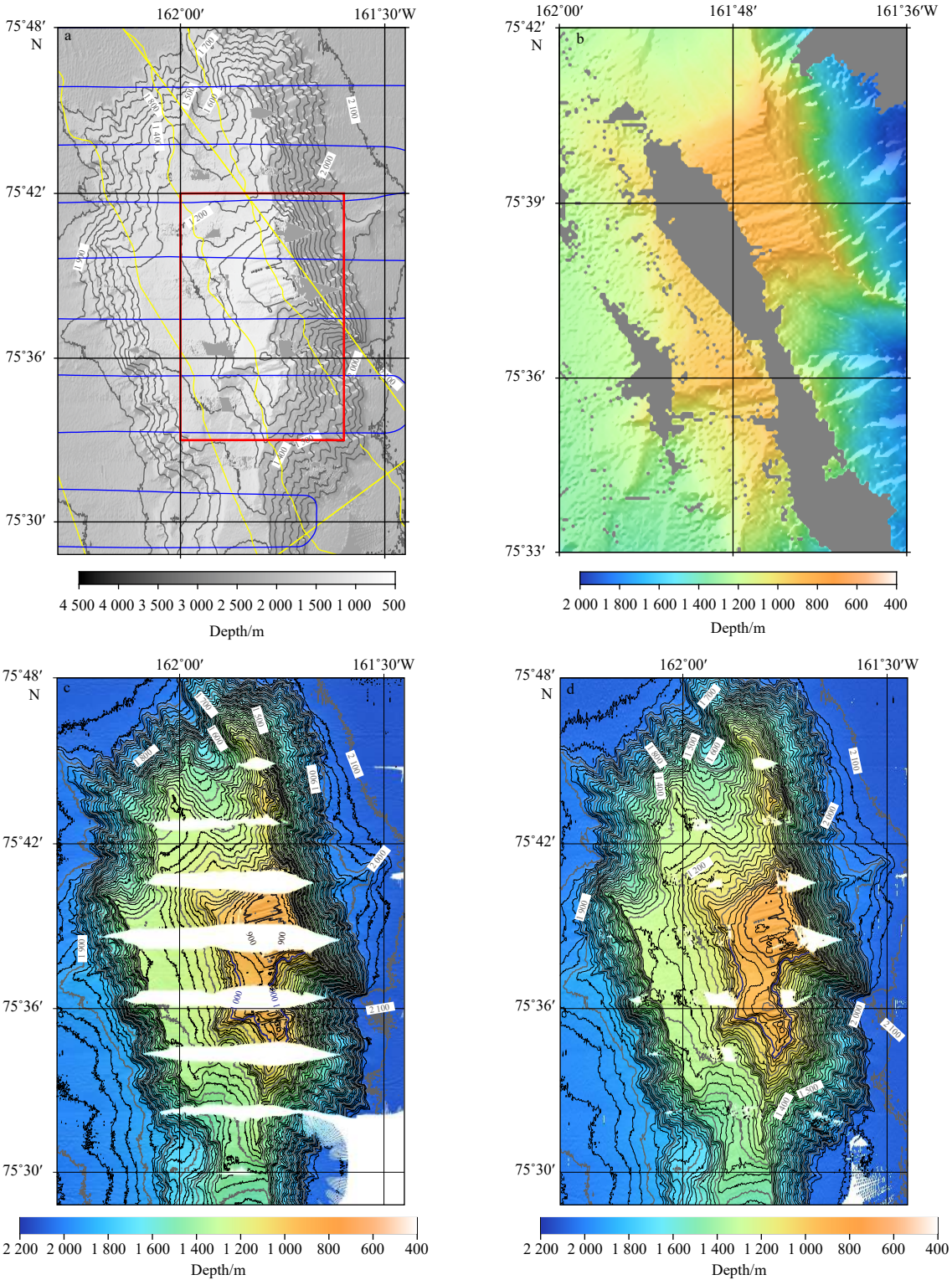

Fig. 2. Multibeam data comparison and compilation. a. Multibeam survey tracks used for compilation and the resulting bathymetric grid. The yellow survey lines are from the four cruises in Dove et al.'s (2014) paper, and the blue lines are the CHINARE-Arc9 survey lines; the red box shows the scope of b whose extent is the same as that in Fig. 3. b. Bathymetric grid of the four cruises in Dove et al.'s (2014) paper reveals only parts of the scours on the crest of the Baoshi Seamount. c. Bathymetric grid of the newly acquired multibeam data during CHINARE-Arc9. d. Compiled bathymetric grid merging the CHINARE-Arc9 data with historical data. All the grid cell sizes are 50 m. The gray areas in b and white areas in c and d are places not covered by multibeam data. The 900-m and 1 000-m isobaths in the scoured area in c and d are indicated by thick black and dark blue lines, respectively.

Seamount is approximately an ellipse in plain view with its long axis along the N–S direction (Fig. 2). Its orientation is similar to those of the other seamounts in the NAP revealed by the IBCAO V3 grid (Jakobsson et al., 2012) (Fig. 1) and other high-resolution

multibeam data (e.g., data from the MGL1112 cruise). The N–S trend of the Baoshi Seamount is also consistent with the trends of faults in the southern NAP revealed by the latest multi-channel seismic profiles (Ilhan and Coakley, 2018), suggesting that the genesis of the Baoshi Seamount may be related to the extension of the NAP.

The Baoshi Seamount has two relatively flat regions, one of which is the flat-topped crest (Fig. 2d). A series of sub-parallel scours are identified on the crest at water depths of 850–1 030 m, with an orientation of about 75°/255° (Figs 2 and 3). The water depth of these scours deepens from north to south. According to their morphology and spacing (Figs 3 and 4), these scours can be roughly divided into two categories, located in the northern and southern zones, respectively (Fig. 3).

3.1 *Northern zone*

The northern zone contains approximately ten scours (Fig. 3), which are roughly surrounded by the 900-m isobath (Figs 2d and 3). The lengths of the scours vary slightly, with the longest length being approximately 2.6 km. The scour lineations are almost equally distributed with an average spacing of about 250 m (Fig. 4a). The longitudinal topographic profile of a typical scour (measured along the bottom of the scour) in this zone (A–A′ in Fig. 3) reveals that the water depths at both ends of the scour are approximately equal (Fig. 5a).

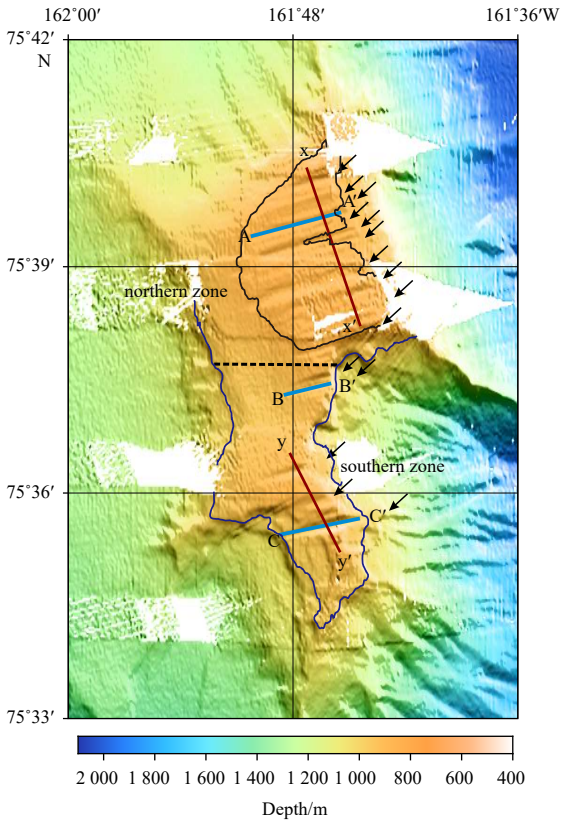

Fig. 3. Glacial scours on the crest of the Baoshi Seamount. The black dashed line marks the boundary between the northern and southern zones. The white areas are places not covered by multibeam data. The black arrows indicate the scours. The 900-m and 1 000-m isobaths are indicated by thin black and dark blue lines, respectively.

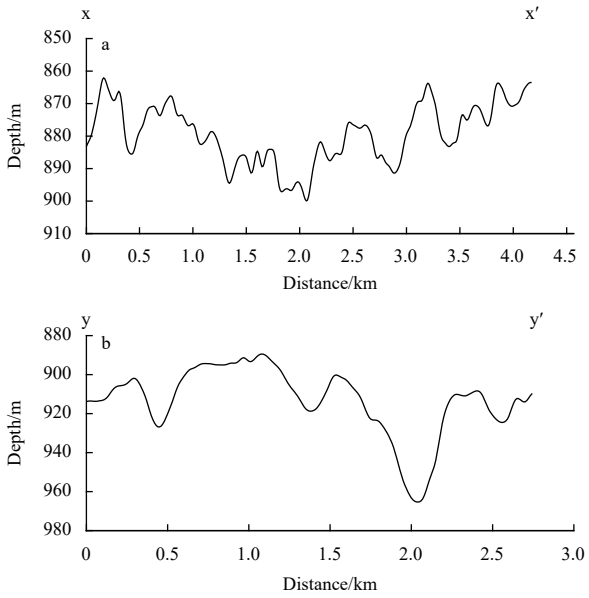

Fig. 4. Cross-sectional topographic profiles of the scour fields of the northern zone (a) and southern subzone of the southern zone (b). The locations are shown in Fig. 3.

3.2 *Southern zone*

At least five scours were identified in the southern zone, ranging in length from 1.2 km to 2.1 km. The spacing between neighboring scours varies greatly, ranging from about 180 m to 1 700 m, which is different from that in the northern zone. The scours in the southern zone can be roughly divided into two subzones. The spacings between neighboring scours in the southern subzone are about 930 m and 650 m (Fig. 4b). The southernmost scour

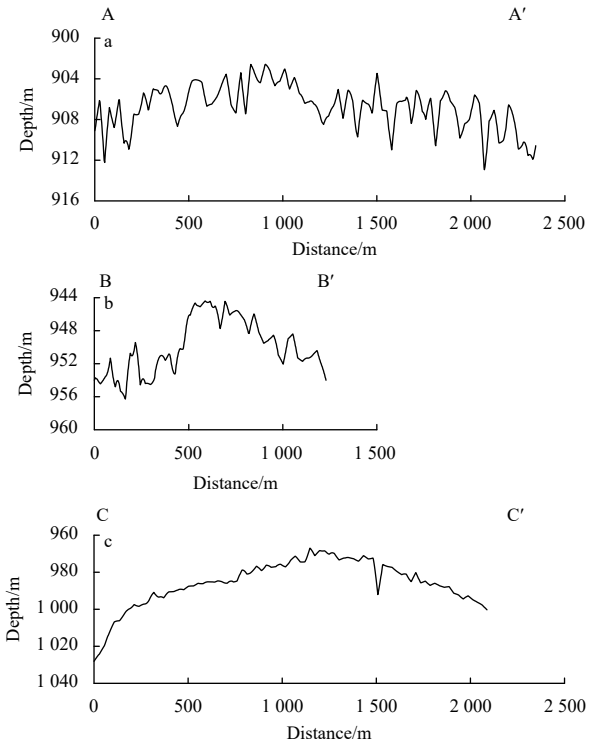

Fig. 5. Longitudinal topographic profiles of three representative scours. The locations are shown in Fig. 3.

widens towards the center and then narrows towards the ends along its SW–NE axis. In comparison, the widths of the other scours in the southern zone increase northeastward. The longitudinal topographic profile of the typical scour in the northern subzone of the southern zone (B–B′ in Fig. 3) shows that the water depths at both ends are approximately 954 m (Fig. 5b), similar to those of the typical profile in the northern zone (Fig. 5a). However, the longitudinal topographic profile of the southernmost scour (C–C′ in Fig. 3) shows that the SW end is approximately 30 m deeper than the NE end (1 030 m vs. 1 000 m, respectively) (Fig. 5c).

4 Genesis of glacial bedforms on the Baoshi Seamount

The scours that developed on the crest of the Baoshi Seamount are not parallel to the survey tracks; thus, the possibility of the scours being artefacts caused by surveying direction can be excluded. In addition to glacial origin, persistent currents can also form lineations on the seafloor. Jakobsson et al. (2008) described the differences between glacial-derived and current-generated lineations. According to these criteria, lineations on the Baoshi Seamount clearly can be ascribed to glacial-origin, as the ridges and troughs of these scours have similar cross-sectional shapes and dimensions (Fig. 4), and they are located on the crest of the seamount, which excludes the possibility that they were generated by persistent currents.

There are two possible factors that can cause glacial linear scours on the deep seabeds, iceberg ploughing (e.g., Dowdeswell et al., 2010) and grounding of the ice sheet/ice shelf (e.g., King et al., 2009; Polyak et al., 2001). Although single-keel icebergs may sometimes generate linear scours, they usually form irregular and chaotic scours (e.g., Figs 6d and 9b of Dowdeswell et al., 2016), which are unlike the sub-parallel scours in the study area. Such sub-parallel linear scours may also be generated by armadas of large icebergs (e.g., Kristoffersen et al., 2004) or multi-keel icebergs (e.g., Wise et al., 2017).

According to the scour orientation, the direction of ice flow may be either from SW to NE or from NE to SW. The longitudinal topographic profiles of the scours in the northern zone and the northern subzone of the southern zone show that the water depths at both ends are almost identical (Figs 5a and b), while that of the southernmost scour shows a slightly larger depth at the SW end (1 030 m) than at the NE end (1 000 m) (Fig. 5c). However, it is difficult to indicate the ice flow direction using only these profiles. In addition, the compiled bathymetric grid that almost covers the entire Baoshi Seamount does not reveal any glacial bedforms that can indicate ice flow direction (such as grounding zone wedges and moraine ridges). Therefore, both directions of ice motion are possible.

If these scours were caused by icebergs, then, where were the icebergs from? The Chukchi Shelf in the southwest seems to be a possible source. MSGLs have been identified in the bathymetric trough east of the Chukchi Rise, some of which are at about 700 m water depth around the shelf break (Dove et al., 2014). If the ice sheet that produced these MSGLs was very thick, then the calved icebergs of this ice sheet might be thick enough to plough over the crest of the Baoshi Seamount. Another possible source is from the east. MSGLs were found at a water depth of about 900 m on the southern Northwind Ridge, southeast of the Baoshi Seamount, with a NWW trend (J900 in Fig. 1) (Jakobsson et al., 2008). These MSGLs were attributed to ice masses from the Laurentide Ice Sheet on northern Canada (Jakobsson et al., 2008). If the linear scours on the Baoshi Seamount were carved by the Laurentide icebergs passing the Northwind Ridge, these icebergs need to undergo a special path of movement, i.e., go to the southwest or northeast of the Baoshi Seamount, and then drift northeastward or southwestward over the Baoshi Seamount. Although this possibility cannot be ruled out, it requires a very special dynamic oceanographic environment, and the possibility of such scenarios is very low. To the northeast of the Baoshi Seamount, there is an area of MSGLs on the Northwind Ridge whose orientation is consistent with that of the scours in the study area (Dove et al., 2014). The water depth of this site reaches up to 700 m. If the paleo ice cap here is thick enough, it may also produce icebergs that can generate scours on the Baoshi Seamount.

Another possibility is that these linear scours are caused by ice sheet/ice shelf grounding. According to the geomorphologic characteristics and zonation of the scours, those from the northern zone indicate that the bottom of the ice shelf is in complete contact with the seabed, so the scours are similar to MSGLs beneath the ice streams. In the southern zone, the scours are deeper and scattered, indicating that only some downward-protruding deep keels of the ice shelf are partially in contact with the seabed. In the Arctic Ocean, similar glacial scours are also thought to be caused by ice shelf grounding (Polyak et al., 2001). Previous studies indicate a Chukchi Ice Sheet existing on the Chukchi Shelf, which may even be connected to the East Siberian Ice Sheet (Niessen et al., 2013) to form the Eastern Siberian-Chukchi Ice Sheet (Dove et al., 2014). A paleo-ice stream moving from SW to NE was identified southwest of the Baoshi Seamount (Dove et al., 2014). These findings make the East Siberian-Chukchi margin similar to the Ross Sea shelf in West Antarctica (Anderson et al., 2014), indicating that ice supply to the Baoshi Seamount may be sufficient by some ancient ice streams from the Chukchi Ice Sheet, possibly forming a thick ice shelf and carving the seabed. In addition, the Northwind Ridge is believed to be affected by the Laurentide Ice Sheet (LIS) (e.g., Polyak et al., 2001; Jakobsson et al., 2008). Although the predominant direction of the LIS ice flow over the southern Northwind Ridge and NAP is NWW (e.g., Dove et al., 2014; Jakobsson et al., 2014), it seems that some paleo ice streams of LIS (such as the M'Clintock ice stream) can affect the Northwind Ridge and Baoshi Seamount in a local SWW direction, thus causing scours with orientations of NEE–SWW on the Baoshi Seamount. Of course, it is also possible that neither of the above two ice streams in opposite directions are not thick enough to ground on the Baoshi Seamount, but the interaction between the two (e.g., convergence) might thicken the ice in the NAP and make it possible to ground on the crest of the Baoshi Seamount as deep as about 1 000 m.

Regardless of which of the above two geneses is correct, the ice at the Chukchi margin to the southwest of the Baoshi Seamount, the southern NAP or the Northwind Ridge northeast of the Baoshi Seamount must be thick enough to produce such scours. Assuming a sea level drop of approximately 130 m during glacial maxima (such as during the Last Glacial Maximum, Lambeck et al., 2014), the minimum ice thickness during glacial maxima (H_{GM}) can be calculated using the formula below, which is similar to Eq. (2) of Anderson et al. (2014).

$$H_{GM} = (\rho_w/\rho_i)(D + \Delta D_{GM}), \quad (1)$$

where ρ_w (1 028 kg/m^3) and ρ_i (910 kg/m^3) are the mean densities of the sea water and ice column, respectively. D is the present-day water depth of the scours on the Baoshi Seamount. ΔD_{GM} is the water depth at glacial maxima minus the present-day water depth (–130 m according the above assumption). For the deepest scour in the study area, D is 1 030 m; thus, H_{GM} is 1 017 m, which means that during glacial maxima, the Chukchi margin to the southwest of the Baoshi Seamount or the southern NAP or the Northwind Ridge northeast of the Baoshi Seamount

was covered by a 1-km-thick ice mass.

5 Conclusions

(1) New multibeam data on the Baoshi Seamount acquired during the 9th Chinese Arctic Research Expedition are presented in this paper. These data fill almost all the blank areas in the multibeam data of the seamount from previous studies. The compiled data revealed much more complete glacial scours on the Baoshi Seamount than previous data.

(2) A series of sub-parallel scours are identified at a water depth of 850–1 030 m on the crest of the Baoshi Seamount (Figs 2 and 3). The scour water depth generally deepens from north to south. According to the morphology and spacing (Figs 3 and 4), these scours can be roughly divided into two categories, located in the northern and southern zones (Fig. 3). Scours in the northern zone are almost equally spaced, while the spacing between neighboring scours in the southern zone varies significantly.

(3) Based on the morphological characteristics of the scours, it is suggested that they are either caused by multi-keel icebergs/armadas of large icebergs, or ice sheet (ice shelf) grounding. In the above two interpretations of bedform genesis, the ice masses that generate the scours may be from the Chukchi continental margin to the southwest or the Laurentide discharge to the northeast of the Baoshi Seamount. The deepest scour suggests that the thickness of the ice mass generating these scours reaches about 1 km.

Acknowledgements

We thank Captain Quan Shen and the crew of the R/V *Xuelong* during the 9th Chinese Arctic Research Expedition. Figures 1–3 were drawn using the GMT package developed by Wessel et al. (2013).

References

Anderson J B, Conway H, Bart P J, et al. 2014. Ross Sea paleo-ice sheet drainage and deglacial history during and since the LGM. Quaternary Science Reviews, 100: 31–54, doi: 10.1016/j.quascirev.2013.08.020

Caress D W, Chayes D N. 2017. MB-System: Mapping the Seafloor. Moss Landing, CA: Monterey Bay Aquariun Research Institute

Donn W L, Ewing M. 1966. A theory of ice ages III. Science, 152(3730): 1706–1712, doi: 10.1126/science.152.3730.1706

Dove D, Polyak L, Coakley B. 2014. Widespread, multi-source glacial erosion on the Chukchi margin, Arctic Ocean. Quaternary Science Reviews, 92: 112–122, doi: 10.1016/j.quascirev.2013.07.016

Dowdeswell J A, Canals M, Jakobsson M, et al. 2016. The variety and distribution of submarine glacial landforms and implications for ice-sheet reconstruction. Geological Society, London, Memoirs, 46: 519–552, doi: 10.1144/M46.183

Dowdeswell J A, Jakobsson M, Hogan K A, et al. 2010. High-resolution geophysical observations of the Yermak Plateau and northern Svalbard margin: Implications for ice-sheet grounding and deep-keeled icebergs. Quaternary Science Review, 29(25–26): 3518–3531, doi: 10.1016/j.quascirev.2010.06.002

Ehlers J, Gibbard P L. 2007. The extent and chronology of Cenozoic Global Glaciation. Quaternary International, 164–165: 6–20, doi: 10.1016/j.quaint.2006.10.008

Grantz A, Hart P E, Childers V A. 2011. Geology and tectonic development of the Amerasia and Canada Basins, Arctic Ocean. Geological Society, London, Memoirs, 35: 771–799, doi: 10.1144/M35.50

Hall J K. 1990. Chukchi borderland. In: Grantz A, Johnson G L, Sweeney J F, eds. The Arctic Ocean region. Boulder: The Geological Society of America, Inc., 337–350, doi: 10.1130/DNAG-GNA-L.337

Hegewald A. 2012. The Chukchi region: Arctic Ocean: tectonic and sedimentary evolution [dissertation]. Bremen: Alfred Wegener Institute-Helmholtz Centre for Polar and Marine Research

Hegewald A, Jokat W. 2013. Relative sea level variations in the Chukchi region-Arctic Ocean-since the late Eocene. Geophysical Research Letters, 40(5): 803–807, doi: 10.1002/grl.50182

Hughes T, Denton G H, Grosswald M G. 1977. Was there a late-würm Arctic Ice Sheet?. Nature, 266(5603): 596–602, doi: 10.1038/266596a0

Ilhan I, Coakley B J. 2018. Meso–Cenozoic evolution of the southwestern Chukchi Borderland, Arctic Ocean. Marine and Petroleum Geology, 95: 100–109, doi: 10.1016/j.marpetgeo.2018.04.014

Jakobsson M. 1999. First high-resolution chirp sonar profiles from the central Arctic Ocean reveal erosion of Lomonosov Ridge sediments. Marine Geology, 158(1–4): 111–123, doi: 10.1016/S0025-3227(98)00186-8

Jakobsson M, Andreassen K, Bjarnadóttir L R, et al. 2014. Arctic Ocean glacial history. Quaternary Science Reviews, 92: 40–67, doi: 10.1016/j.quascirev.2013.07.033

Jakobsson M, Mayer L, Coakley B, et al. 2012. The international bathymetric chart of the Arctic Ocean (IBCAO) version 3. 0. Geophysical Research Letters, 39(12): L12609, doi: 10.1029/2012GL052219

Jakobsson M, Nilsson J, Anderson L, et al. 2016. Evidence for an ice shelf covering the central Arctic Ocean during the penultimate glaciation. Nature Communications, 7: 10365, doi: 10.1038/ncomms10365

Jakobsson M, Polyak L, Edwards M, et al. 2008. Glacial geomorphology of the central Arctic Ocean: The Chukchi borderland and the Lomonosov ridge. Earth Surface Processes and Landforms, 33(4): 526–545, doi: 10.1002/esp.1667

King E C, Hindmarsh R C A, Stokes C R. 2009. Formation of mega-scale glacial lineations observed beneath a West Antarctic ice stream. Nature Geoscience, 2(8): 585–588, doi: 10.1038/ngeo581

Kristoffersen Y, Coakley B, Jokat W, et al. 2004. Seabed erosion on the Lomonosov Ridge, central Arctic Ocean: A tale of deep draft icebergs in the Eurasia Basin and the influence of Atlantic water inflow on iceberg motion?. Paleoceanography and Paleoclimatology, 19(3): PA3006, doi: 10.1029/2003PA000985

Lambeck K, Rouby H, Purcell A, et al. 2014. Sea level and global ice volumes from the Last Glacial Maximum to the Holocene. Proceedings of the National Academy of Sciences of the United States of America, 111(43): 15296–15303, doi: 10.1073/pnas.1411762111

Mercer J H. 1970. A former ice sheet in the Arctic Ocean?. Palaeogeography, Palaeoclimatology, Palaeoecology, 8(1): 19–27, doi: 10.1016/0031-0182(70)90076-3

Niessen F, Hong J K, Hegewald A, et al. 2013. Repeated Pleistocene glaciation of the East Siberian continental margin. Nature Geoscience, 6(10): 842–846, doi: 10.1038/ngeo1904

Ottesen D, Dowdeswell J A. 2009. An inter–ice-stream glaciated margin: Submarine landforms and a geomorphic model based on marine-geophysical data from Svalbard. GSA Bulletin, 121(11–12): 1647–1665, doi: 10.1130/B26467.1

Polyak L, Darby D A, Bischof J F, et al. 2007. Stratigraphic constraints on late Pleistocene glacial erosion and deglaciation of the Chukchi margin, Arctic Ocean. Quaternary Research, 67(2): 234–245, doi: 10.1016/j.yqres.2006.08.001

Polyak L, Edwards M H, Coakley B J, et al. 2001. Ice shelves in the Pleistocene Arctic Ocean inferred from glaciogenic deep-sea bedforms. Nature, 410(6827): 453–457, doi: 10.1038/35068536

Shipp S, Anderson J B, Domack E W. 1999. Seismic signature of the Late Pleistocene fluctuation of the West Antarctic Ice Sheet system in the Ross Sea: a new perspective, Part I. Geological Society of America Bulletin, 111: 1486–1516, doi: 10.1130/0016-7606(1999)111<1486:LPHROT>2.3.CO;2

Stein R, Matthiessen J, Niessen F, et al. 2010. Towards a better (litho-) stratigraphy and reconstruction of Quaternary paleoenvironment in the Amerasian Basin (Arctic Ocean). Polarforschung, 79(2): 97–121

Wessel P, Smith W H F, Scharroo R, et al. 2013. Generic mapping tools: Improved version released. EOS, 94(45): 409–410, doi: 10.1002/2013EO450001

Wise M G, Dowdeswell J A, Jakobsson M, et al. 2017. Evidence of marine ice-cliff instability in Pine Island Bay from iceberg-keel plough marks. Nature, 550(7677): 506–510, doi: 10.1038/nature24458